SAND2008-2736C

# A Thermal Model for Thermal Batteries

***Nicholas D. Streeter, David Ingersoll, Dean Dobranich***
Power Source Technology Group
Sandia National Laboratories
Albuquerque, NM 87185, USA
ndstree@sandia.gov

***Eivind Listerud***
Defense and Space Power
EaglePicher Technologies
Joplin, MO 64801, USA

**Abstract:** *An axisymmetric finite element code was developed at Sandia National Laboratories to predict temperature and heat flux throughout the thermal battery as a function of time. This thermal model was evaluated using temperature waveforms acquired from highly instrumented thermal batteries built and tested at SNL. The model has also been used to investigate the sensitivity of various material parameters to the thermal performance of the battery, allowing for a better understanding of the critical thermal parameters of the design.*

**Keywords:** thermal batteries; modeling; thermal management.

## Introduction

The management of heat flux is a critical parameter in the design of molten salt thermal batteries. It is important to understand the temperature distribution within the battery as a function of time to determine when the electrolyte is molten. Maximum exposure temperatures are also of importance to ensure that thermally sensitive materials are not degraded.

Sandia National Laboratories (SNL) work with thermal modeling of thermal batteries dates back to the late 1970s with the development a finite difference code for modeling a quarter section of a thermal battery.[1] In the 1980s, this code was expanded upon by Royal Aerospace Establishment[2] and became a useful design tool in thermal battery development at SNL. Because of the limitations and inefficiencies of the RAE code, a new finite element code was developed at SNL by Dobranich in 1995. This code contains many improvements compared to previous codes, including robust adjustable time-step control and improved input flexibility to allow modeling of various battery designs. More recently, this latest code has been supplemented with various pre- and post-processing tools[3] for increased ease of use, and it is the model used for the work presented in this paper.

## Experimental

*Test Setup:* Eleven replicates of highly instrumented thermal batteries were constructed and tested at SNL. These units were instrumented with internal and external thermocouples (TCs) to provide a temperature waveform at select locations as a function of time. Each battery consisted of 10 Li(Si)/LiCl-KCl/$FeS_2$ electrochemical cells (electrolyte m.p. 352°C). An Fe/$KClO_4$ heat pellet and two current collectors (SS or graphite) were placed between each cell. Additional heat pellets were placed at the top and bottom of each stack along with insulation materials. The stack was wrapped with insulation and placed into a hermetically sealed stainless steel container. Details of the battery construction and instrumentation are documented in Paper No. 7.2 included in these conference proceedings.

*Model Setup:* A planar mesh was generated to represent the test battery configuration. The mesh contained 4557 nodes making up 4320 rectangular elements. Each element was assigned material properties of one of 13 materials. During the computational simulation, the battery is represented by the planar mesh revolved about an axis, resulting in an axisymmetric model. Boundary conditions allow for free convection and thermal radiation from all external surfaces to replicate the experimental test setup. The mesh used is shown in Figure 1.

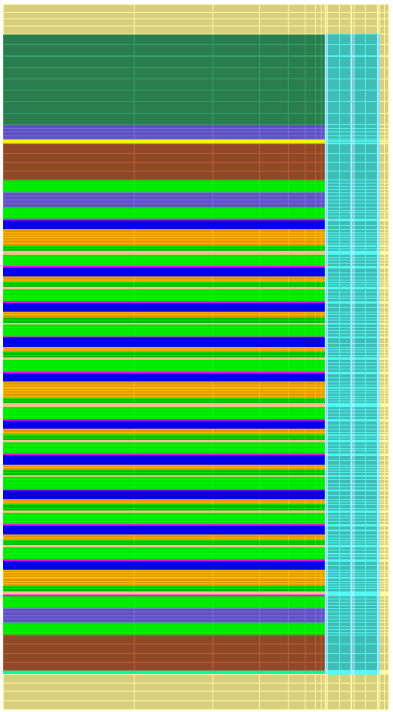

**Figure 1.** Mesh of thermal battery.

*Material Properties:* The material properties used in this model are density, heat capacity, and thermal conductivity, as well as solidus/liquidus temperatures and latent heat of fusion for components that undergo a phase change. Material properties were gathered from a variety of internal and external sources, with some measured to higher fidelity than others. Most properties are represented as a function of temperature, however, some properties are assumed to be constant because of lack of available data. Ideally, one

would have all properties as a function of temperature and state of battery discharge.

*Sensitivity Analysis:* It is of interest to know which material properties have the largest impact on battery performance. The initial approach varied each of 29 different model parameters by five percent to determine which property had the most influence on the temperature profile at various locations within the battery. These included heat capacity, thermal conductivity, and phase change parameters. Additionally, the calorific output of the heat pellet was varied. This approach varied only one parameter at a time and assumed that the result of each perturbation was independent of the others.

## Results and Discussion

*Experimental Data:* The temperature profile as a function of time for a given TC location varied slightly from battery test to test. Differences could be attributed to battery-to-battery variability, or they could be caused by the variation in the data collection configuration. The test data used for model comparison were comprised of an average of the four highest fidelity tests. These tests included the fastest responding TCs and did not include hardware filtering during data capture.

*Model Validation:* To characterize the computational model, the model output was compared to the test data collected for the given battery configuration. Virtual TC locations were selected at nodes of interest within the mesh corresponding to actual TC locations. The resulting temperature waveforms were then compared. Figure 2 shows seven selected TC locations within the test battery.

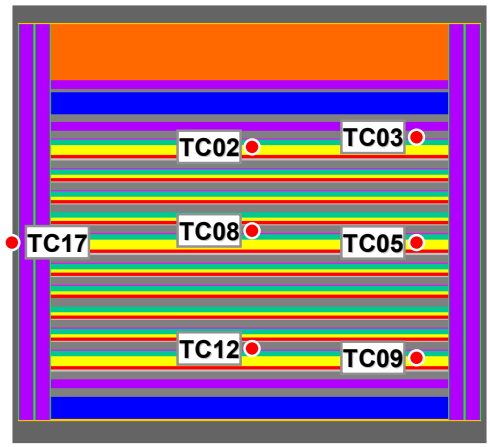


**Figure 2.** Location of thermocouples in battery.

Comparisons of waveforms at the TC locations are shown in Figures 3-10. TCs shown include those at the cathode/collector interface and those in the separator pellet. Once a given cell has reached equilibrium after the initial heat pellet burn, the cathode/collector and separator TC profiles for the same location in a cell are effectively equivalent.

Some features should be noted when comparing the experimental and model data. Observe the temperature plateaus starting at approximately 12 minutes in Figures 3-8. These are a result of an electrolyte phase change. Increased ionic resistance occurs when the electrolyte liquidus temperature is reached, so this time of onset is of interest. Once the electrolyte reaches solidus temperature, ionic transfer across the separator stops, and the battery life has ended.

Although battery performance life has ended, it is useful to understand the model performance once the liquidus temperature is reached. This can help in understanding the electrolyte phase change during early battery life, when the phase change occurs more rapidly. The difference in the duration of electrolyte freeze may be due to inaccurate material properties or possibly caused by a buildup of reaction products within the various battery layers. The thermal model does not factor in these changes.

Model assumptions may have led to some slight mismatches in experimental versus model waveforms. The higher experimental temperature observed in Figure 4 during the first minute may be due to the heat imparted by the battery igniter. The model does not include this.

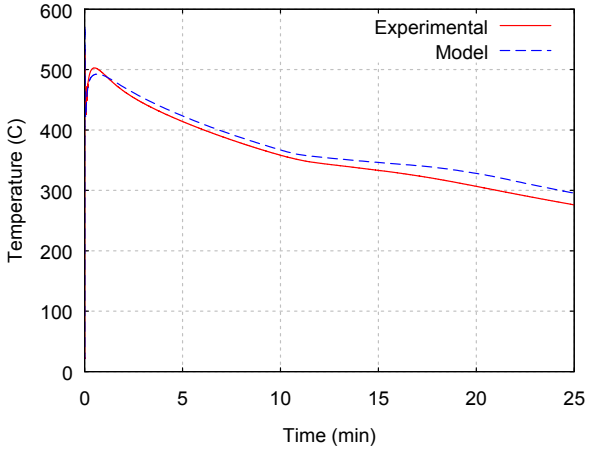


**Figure 3.** Cell 1, edge; cathode/collector interface (TC03).

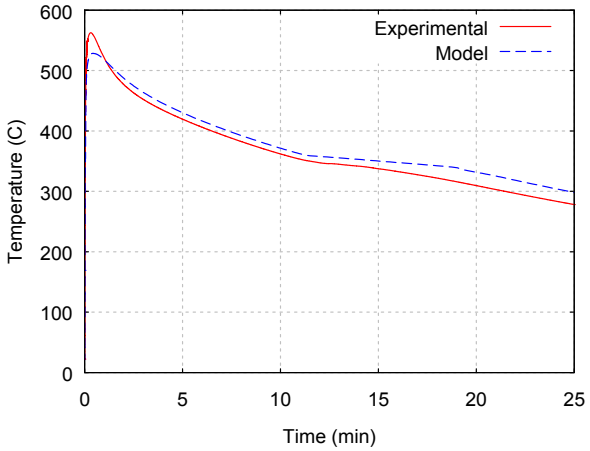


**Figure 4.** Cell 1, center; middle of separator pellet (TC02).

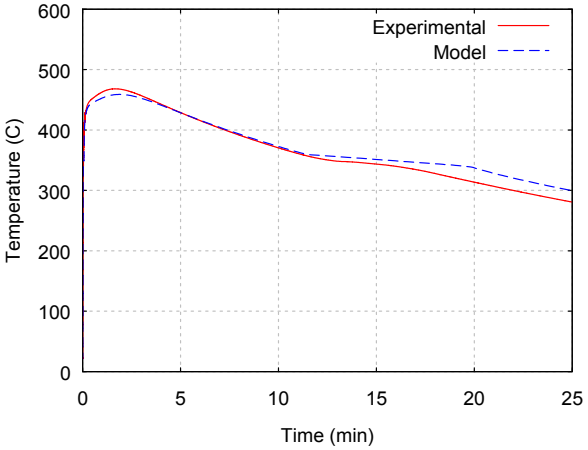


**Figure 5.** Cell 5, edge; middle of separator pellet (TC05).

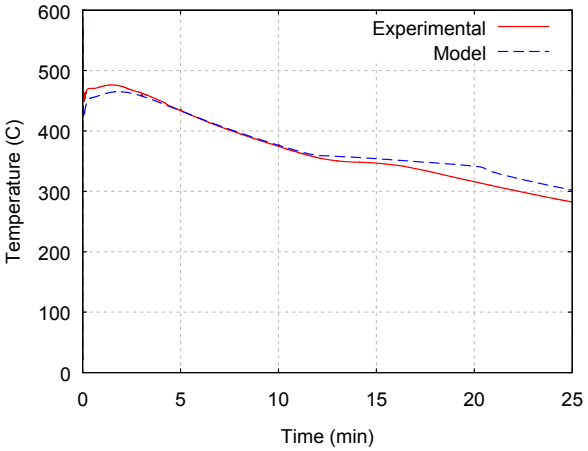


**Figure 6.** Cell 5, center; cathode/collector interface (TC08).

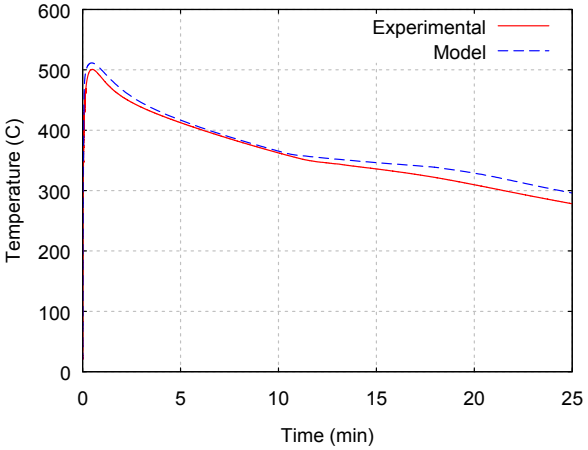


**Figure 7.** Cell 10, edge; middle of separator pellet (TC09).

The model also assumes simultaneous activation of all heat pellets within the battery stack. The heat pellet activation was specified at 0.4 seconds, and burn time was assumed to be 0.2 seconds. An example of rise time behavior is shown in Figure 10. Note the temperature plateau seen during

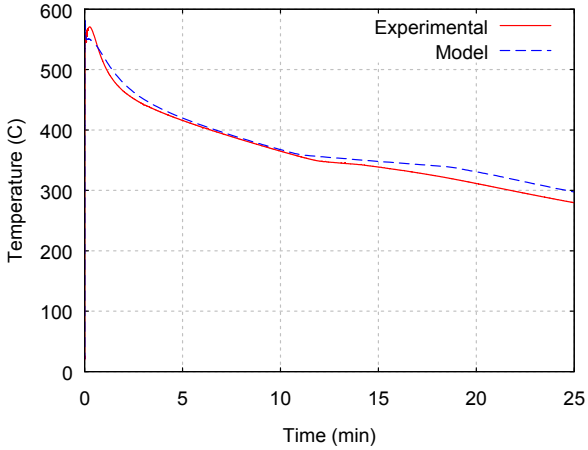


**Figure 8.** Cell 10, center; cathode/collector interface (TC12).

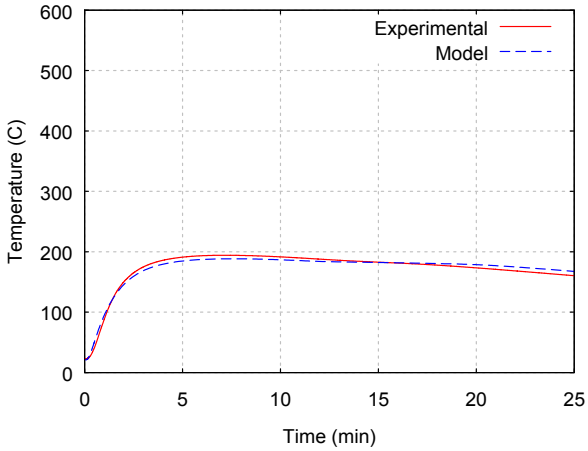


**Figure 9.** Cell 5, outside surface of battery case (TC17).

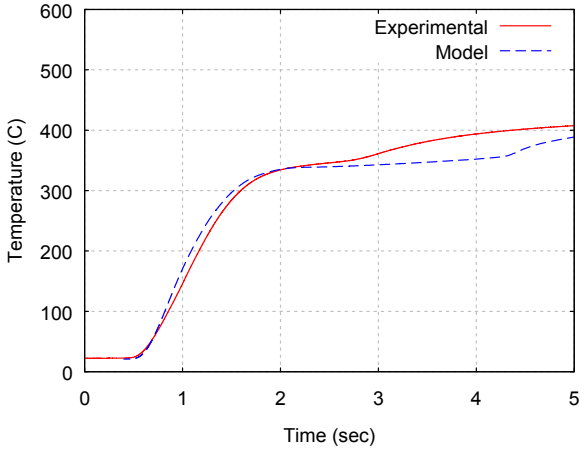


**Figure 10.** Cell 5, edge; middle of separator pellet (TC05).

electrolyte phase change. Differences are likely due to inaccurate material properties and/or TC response time.

*Sensitivity Analysis:* After gaining confidence in the predictive capability of the model for this battery configuration, the sensitivity of certain input parameters

was investigated. Figure 11a highlights the dominant factors in a difference plot of the nominal temperature profile and the varied temperature profile at a virtual TC location at the center of the separator of cell 5. Figure 11b shows this plot zoomed to observe behavior during rise time. Each parameter was varied independently from the others. The calorific output of the heat pellet was increased by five percent. The remaining parameters were decreased by five percent. The onset of the electrolyte phase change is the time when the temperature difference of all variations nears zero (~720 sec).

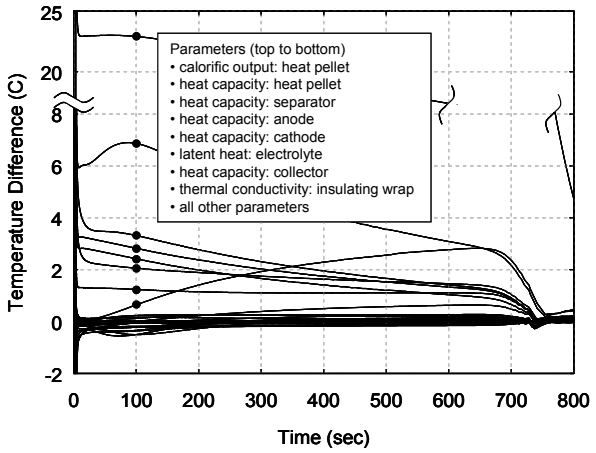


**Figure 11a.** Difference plot of nominal model temperature profile and parameter varied temperature profile within separator pellet.

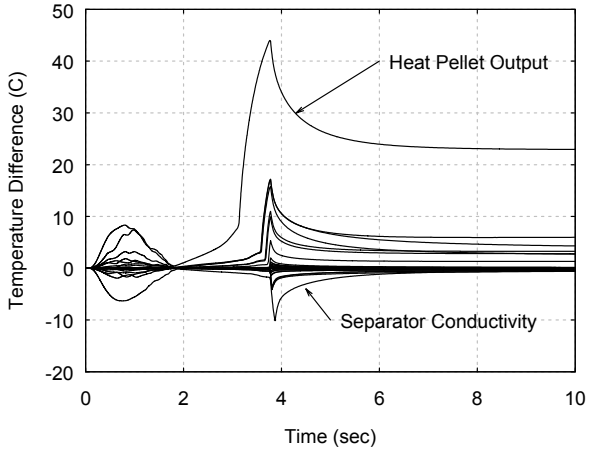


**Figure 11b.** Same as Figure 11 with different axes.

Variation in the calorific output of the heat pellet had the greatest effect on the temperature difference within the battery. The heat capacity of the battery materials in the stack had the next greatest impact on the temperature profile of the battery. These include the heat capacities of the heat, separator, anode, and cathode pellets. The latent heat of fusion of the electrolyte followed. The thermal conductivity of the insulating wrap starts with minimal effect, but the temperature difference gradually increases and has its greatest impact close to the time of electrolyte freeze. Most other parameters had little impact on the temperature profile using the 5% change.

Since there is a known energy input into the system during battery activation, the effect of heat input and heat capacity of cell stack materials logically have the greatest effect on the temperature profile in the battery over the majority of activated battery life. During the first few seconds after battery activation, changes in temperature profile can be observed by varying material thermal conductivities, but this effect fades within 10 seconds, with the exception of the insulating wrap as discussed above. (The effect of changing the solidus/liquidus range is not shown because the timing of melt and freeze is not well presented using the difference plot method.)

## Conclusions

This model can be used to optimize the thermal management of a thermal battery prior to prototyping, resulting in fewer build iterations. Also, raw material and processing costs may be reduced by refining material specifications to align with critical thermal parameters.

This thermal model agrees closely with experimental data gathered for the given thermal battery configuration. To enhance model output, the following improvements should be considered: 1) increased precision and accuracy of material properties measurements, acquiring all properties as a function of temperature; 2) inclusion of burn rate parameters for both heat pellets and heat paper; and 3) a more in-depth approach to sensitivity analysis, including the correlation of variables and quantification of sensitivity coefficients for all parameters.

## Acknowledgements

Results from instrumented thermal batteries discussed in this paper were conducted under a SNL Work for Others contract with EaglePicher Technologies, with funding provided by the Missile Defense Agency (MDA).

Sandia is a multi-program laboratory operated by Sandia Corporation, a Lockheed Martin Company, for the United States Department of Energy's National Nuclear Security Administration under contract DE-AC04-94AL85000.

## References

1. D.M. Bush and R.L. Hughes, "A Thermal Model of a Thermal Battery," Sandia National Laboratories, SAND79-0834, 1979.
2. J. Knight and I. McKirdy, "The Prediction and Measurement of Thermal Battery Internal Temperatures During and After Activation," 15th International Power Sources Symposium, 1986.
3. H.W. Papenguth, J.R. Weatherby, D. Dobranich, T.C. Barrentine, P.F. Chavez, and L.J. Lehoucq, "Design-Simulation Tool for Thermal Analysis of Thermal Batteries," The Electrochemical Society, 202nd Meeting, 2002.